Macromolecules

Volume 27, Number 15 July 18, 1994

Catalytic Synthesis of Poly(ethylene terephthalate-*co*-oxybenzoate) Systems via the Melt Polyesterification Route: Copolyesterification Kinetics†

J. Mathew, R. S. Ghadage, and S. Ponrathnam*

Polymer Science and Engineering Group, Chemical Engineering Division, National Chemical Laboratory, Pune 411 008, India

S. D. Prasad*

Physical Chemistry Division, National Chemical Laboratory, Pune 411 008, India

Received March 5, 1993; Revised Manuscript Received May 9, 1994•

ABSTRACT: Kinetics of copolyesterification between poly(ethylene terephthalate) and 4-acetoxybenzoic acid (PET/ABA) in the melt has been analyzed using a phenomenological approach. A parallel second-order reaction sequence neatly summarizes catalyzed and uncatalyzed homopolyesterifications of 4-acetoxy benzoic acid (ABA) as well as the PET/ABA copolyesterification. Single stage kinetics fits the data reasonably well since the length of oxybenzoate sequences in the copolyester chain seldom exceed 5. Close correspondence exists between the kinetic parameters determined for the first stage of 4-acetoxybenzoic acid homopolyesterification, prior to oligomer precipitation, and those obtained in the present study through a least squares procedure. A Gauss–Legendre quadrature numerical procedure, used to compute the amount of acetic acid produced, is very efficient for comparison with experiments. Rate constants for copolyesterification are found to be several times lower than those of ABA polyesterification. The kinetics data support the formation of randomized blocks in the PET/oxybenzoate chain. The thermal data give support to this as well as to liquid crystallinity in a specific copolyester composition range. We also fitted a more elaborate complex kinetic model in which all the possible reaction sequences of importance have been explicitly accounted for. The complex rate model deviates from the simplified model by a marginal correction term. The simplified rate model directly results when we truncate the number of reaction events to only those few significant ones.

Introduction

Discovery of wholly aromatic main chain lyotropic liquid crystalline polymers in the research laboratories of DuPont[1] triggered intensified research directed toward the evolution of main chain thermotropic systems. Here, a number of strategies have been embraced to bring down the aspect ratio in wholly aromatic systems so as to cause a lowering of the liquid crystalline transition temperatures to such a level that organized phases are displayed prior to degradation.[2] Another and perhaps only marginally less significant approach has been to increase the aspect ratio in thermoplastic systems through the incorporation of rigid and colinear structural moieties.[3] The commercialized systems in the former category are copolyesters from (i) 4-hydroxybenzoic acid, 4,4′-dihydroxybiphenyl, and terephthalic acid (Dart Co.) and (ii) 4-hydroxybenzoic acid and 6-hydroxy-2-naphthoic acid (Celanese Corp.). The most prominent system pertaining to the latter is the copolyester of poly(ethylene terephthalate) and 4-acetoxybenzoic acid (Eastman Kodak Co.). These systems have predominantly random structures. The stirring academic research in this field has overwhelmingly stressed the synthesis of novel mesogens, with aspect ratios ranging between 3 and 6.4, which are coupled through aliphatic spacers to form ordered rigid rod–flexible spacer type polymer systems. The most significant of these have been the substantial contributions of Lenz's group relating to the synthesis of a sweeping variety of thermotropic structures and establishing thermal property correlations.[4–15]

Copolyesters of poly(ethylene terephthalate) and 4-acetoxybenzoic acid (PET/oxybenzoate) were synthesized by Jackson et al. through high temperature melt transesterification. However, intricate details pertaining to the polyesterification kinetics have remained unexamined. In this system, insertion of 4-oxybenzoate moieties, with stiff rodlike conformations, into flexible PET chains fosters the development of thermotropic character within a definitive range of copolyester composition. Structural elucidations have generated conflicting data for the system. The ^{13}C NMR[16] and high temperature X-ray diffraction[17]

* Authors for correspondence.
† NCL Communication No. 5732.
• Abstract published in *Advance ACS Abstracts*, June 15, 1994.

0024-9297/94/2227-4021$04.50/0

point to a random organization of PET and oxybenzoate units along the copolyester chain. Thermal analyses[18-20] have implied an inclination toward a nonrandom assembly. Similarly, optical and electron microscopy examinations,[21] coupled with data from X-ray and conventional electron microscopy, endorse the existence of ordered domains or lamellar 4-oxybenzoate blocks in the PET/80 ABA copolyester. The cooling of an annealed melt is known to trigger a biphasic structure.[22] By complementing electron microscopy imaging with optical microscopy, Sawyer[23] has shown that the PET/60 ABA copolyester is oriented and crystalline, implying that the fiber matrix is oriented and is rich in the oxybenzoate. Thus, characterization of PET/ABA copolyesters by many research groups using different techniques seems to have generated a conflicting set of data relating to the structural features.

The foregoing discussion clearly shows that while there is considerable information available on the structure–property aspects of PET/ABA systems, there is a total lack of kinetic information. This work is an attempt at formulating a plausible kinetic model for the PET/ABA melt copolyesterification reaction.

There is a need to understand copolyesterification kinetics since a precise control of the polymer properties and process productivity is one of the key issues in designing or optimizing the melt transesterification process. To this end, a detailed investigation of the synthesis of poly(4-oxybenzoate) through melt transesterification of 4-acetoxybenzoic acid was conducted.[24] A notable observation was that even though the activation energy for the catalyzed homopolyesterification of ABA was higher than that for the uncatalyzed reaction, the considerably lower free energy of activation in the former case led to a significant net rate acceleration. Thus, the predominant and significant role of entropy of activation outweighing the enthalpy increase (compensation effect) was demonstrated. The present system forms a companion study. Here, it is hoped to employ the kinetic information already gained to simplify the understanding of a more complex kinetics. It is of interest to find out whether such a compensation effect is operative in the copolyesterification between PET and 4-acetoxybenzoic acid as well, since a significant extent of ABA homopolyesterification may also take place.

The work was carried with the following objectives: (i) to develop a mathematical model capable of analyzing the system which involves two competitive parallel reactions generating a common byproduct (acetic acid); (ii) to determine the kinetic order with respect to the concentrations of both the 4-acetoxybenzoic acid monomer and PET segments; (iii) to determine the ratio of kinetic rate constants (reactivity ratios) for the two processes; (iv) to predict the rate of acetic acid production by assuming a random sequence distribution for the copolyester; (v) to determine whether a procedure analogous to those involved in modeling solution kinetics can adequately describe melt polyesterification kinetics from a phenomenological point of view; (vi) to achieve this objective a simple model as well as a more elaborate complex rate model have been proposed.

The work is presented as follows: At first a mathematical model capable of analyzing systems in which two competitive reactions occur is considered. The kinetic order is determined at various temperatures for both catalyzed and uncatalyzed runs to see whether kinetic order changes with catalyst. It will also be shown that oxybenzoate precipitation is not appreciable so as to warrant the introduction of a two stage kinetic model with precipitation. It will be also shown that the kinetic constants for ABA homopolyesterification as observed in copolyesterification correspond to the first stage before precipitation in homopolyesterification of ABA, when studied alone.[24] The temperature behavior of the kinetic constants for oxybenzoate homopolyesterification does not show any compensation effect in the presence of PET. A realistic reaction model accounting for all the possible reaction sequences after PET chain slicing will be shown to result in an overall kinetic expression which reduces to a simple kinetic model. Lastly, physico-chemical characterization of the PET/ABA copolyesters synthesized in the study is considered, using dilute solution viscosity, optical microscopy, and differential scanning calorimetry.

Experimental Section

Materials. 4-Acetoxybenzoic acid was synthesized and characterized as described earlier.[24] Poly(ethylene terephthalate) (1676 μm), of intrinsic viscosity 0.58 (M/S Century Enka Private Ltd., Pune, India), was used as received.

Reactor Fabrication. A 250-mL glass lined electrically heated reactor[24] was used for synthesis and the melt transesterification kinetic investigations.

Preparation of Copolyesters. The transesterifications were conducted with the objective of analyzing the copolyesterification kinetics in the initial cycle of the reaction wherein the distillation of the side product, acetic acid, was complete under atmospheric pressure. Transesterifications were conducted to generate a series of copolyesters of varying compositions. Polyesterification kinetics were investigated at three compositions PET/50 ABA, PET/60 ABA, and PET/70 ABA comprising 50:50, 40:60, and 30:70 mol % of PET:ABA. PET melted around 256 °C and degraded around 320 °C on maintaining isothermally for 15 min at atmospheric pressure. The isothermal temperatures chosen for the kinetic estimates were 260, 275, 290, and 305 °C, respectively. A dry nitrogen blanket was maintained throughout the experiments to prevent oxidative degradations. The rate of evolution of byproduct, acetic acid, was monitored volumetrically to estimate the kinetic parameters. Dibutyltin oxide, the most suitable catalyst in the homopolyesterification of 4-acetoxybenzoic acid,[24] was used for this transesterification reaction. *This has hitherto not been evaluated as a catalyst for the synthesis* of PET/ABA systems. In the study relating to polyesterification of 4-acetoxybenzoic acid complication arose from the precipitation of oligomers with an average degree of polymerization equaling or exceeding 6. In this study the kinetic evaluation is simplified since the copolyesters of varying compositions formed remained molten at the temperatures employed in the kinetic study. ABA lost due to sublimation was monitored and was found to be less than 0.075 mol % of the initial reactant charged. Therefore, no correction was made for the loss in the overall mass balance. The purity of acetic acid formed was also estimated at different isothermal kinetic temperatures. This was found to be 95% at 275 °C and 92% at 295 and 305 °C, respectively. The maximum conversion noted, based on moles of acetic acid, was 80%. The light tan and opaque copolyesters were powdered, and acetone was extracted to remove unreacted 4-acetoxybenzoic acid, if any, prior to characterization.

Measurements. Inherent viscosities were measured at 25 °C using an Ubbelohde viscometer in 60:40 v/v phenol–tetrachloroethane at a concentration of 0.5 gm/dL.

The copolyesters were observed under a polarizing microscope equipped with a Koffler hot stage. A small amount of copolyester was mounted between a slide and cover slip and was then heated on the stage at a constant rate. The copolyesters were observed under crossed polarizers.

Thermal transitions were obtained with a Mettler DSC 30 apparatus interfaced with a thermal analysis data station under a nitrogen atmosphere using a sample size of 10–15 mg. A heating rate of 10 °C/min was employed in all the cases. Indium was used to calibrate the enthalpy values. Three metals (In–Pb–Zn) were used to calibrate the temperature scale. Samples were analyzed in the temperature range 40–385 °C in both heating and cooling cycles.

Results and Discussion

In our earlier study it was observed that second-order kinetics was valid for polyesterification of ABA. It is assumed that in the present analysis the same mechanism is valid for homopolyesterification. For treating the second reaction it was assumed that the 4-acetoxybenzoic acid (ABA) monomers approach a PET homopolyester by random Brownian diffusion, followed by a reaction. This can also be treated as a second-order reaction between a PET segment and an ABA monomer.

In the homopolyesterification of ABA[24] a tacit assumption was made that oligomers up to $\overline{DP} = 5$ were in the melt. However we do not consider the possibility of oligomers other than the ABA monomer getting incorporated into the PET chain (mainly from probability considerations based on actual concentrations of these oligomers) even though the end group reactivity of these oligomers is not negligible. Otherwise the kinetic analysis will become intractable. The only guideline for justifying this procedure is the extent of the agreement with experiment.

Kinetics and Mechanism. The reactions which occur when PET and 4-acetoxybenzoic acid are heated together or maintained isothermally at temperatures in excess of the isotropization temperature of crystalline PET may be visualized as depicted in Figure 1. PET chain cleavage occurs principally through the step represented in Figure 1a. PET cleavage with 4-acetoxybenzoic acid (ABA) results in formation of PET segments terminated with carboxylic acid end groups (terephthalic acid end groups) (A) and PET segments terminated with acetoxy end groups (acetoxybenzoyl end groups) (B) as per the mechanism described earlier for cleavage of PET with terephthalic acid.[25] However, acetic acid is not generated in this step, which should be borne in mind in computing its generation rate. The PET cleavage can also proceed through ester–ester exchange. The rate of this reaction is far too slow to be of any significance[26] to the overall process under consideration here.

Segment A and segment B react to re-form the PET chain with insertion of an oxybenzoate unit and generation of acetic acid, as shown in Figure 1b. The other possible reactions of segments A and B are also depicted in Figure 1c–e. These reactions include (i) addition of acetoxybenzoic acid to segment A having a terephthalic acid end group (Figure 1c) to form segment (AO), (ii) addition of acetoxybenzoic acid to segment B having an acetoxybenzoate end group (Figure 1d) to form segment (BO), and (iii) coupling of segment AO and segment BO to re-form the chain with insertion of higher oligomers of oxybenzoate units (Figure 1e). In short, the mechanism shown in Figure 1c–e is the insertion of oxybenzoate oligomers (dimer, trimer, ...) into the PET chain. In other words, this can be visualized as formation of oligomers of oxybenzoate (i.e. homopolyesterification)[24] by addition of acetoxybenzoic acid to itself and insertion of these oligomers into the PET chain via a mechanism similar to (a) and (b) (Figure 1).

The kinetic model is developed by considering these two major competing reactions, i.e. (i) homopolyesterification of 4-acetoxybenzoic acid and (ii) insertion of acetoxybenzoic acid or oligomeric acetoxybenzoic acid into the PET chain.

Development of a Simple Kinetic Model. The entire gamut of reactions, if accounted for, will result in very complex and unwieldly rate expressions,[27] which will have very little practical utility. Hence in the following section we consider a simple reaction model (to be replaced by a complex one later). The reactions leading to the formation of copolyester are (i) homopolyesterification, (ii) PET chain cleavage by 4-acetoxybenzoic acid or oligomers of oxybenzoate, and (iii) PET chain re-formation with insertion of an oxybenzoate unit. These major reactions are

$$\mathrm{ABA} + \mathrm{ABA} \xrightarrow{k_h} (\mathrm{ABA})_2 + \mathrm{CH_3COOH} \qquad \text{(I)}$$

$$\mathrm{PET} + \mathrm{ABA} \xrightarrow{k_s} \mathrm{A} + \mathrm{B} \qquad \text{(II)}$$

$$\mathrm{A} + \mathrm{B} \xrightarrow{k_{f_1}} \mathrm{PEOT} + \mathrm{CH_3COOH} \qquad \text{(III)}$$

Here, k_h, k_s, and k_{f_1} are the rate constants of homopolyesterification, PET chain scission, and chain re-formation with insertion of an oxybenzoate unit, respectively. Species A and B are intermediate in nature. These are generated as in eq II and are consumed in the reaction as per eq III. The concentrations of A and B cannot be directly monitored for the kinetic evaluation. We now add up reaction schemes II and III. The result is the overall reaction given by (IV). This reaction network forms a

$$\mathrm{PET} + \mathrm{ABA} \xrightarrow{k_c} \mathrm{PEOT} + \mathrm{CH_3COOH} \qquad \text{(IV)}$$

parallel second-order reaction sequence, the kinetics of which is indeed very simple, if we invoke the steady state assumption for the rate of production of A and B, i.e. $d[A]/dt = d[B]/dt = 0$ (see Appendix A). Hence the key assumption is that the chain scission of PET is slow in comparison to the reaction between A and B (reaction 1b in Figure 1), so that overall second-order kinetics follows in a direct manner (Appendix A). Equations I and IV form the kinetic model for the reaction, where the rate constant of copolyesterification, k_c, is the net result of rate constants k_s and k_{f_1}.

$[ABA] = a - x$; $[PET] = b - y$. Here a and b denote the initial concentration of monomer ABA and PET repeat units (without an ABA unit insertion). k_h, k_c, x, y, $(ABA)_2$ and PEOT respectively denote the kinetic constants, moles of acetic acid produced, moles of virgin PET segments cleaved, homopolyester, and copolyester. x denotes the total moles of acetic acid produced through both the reaction channels. The rate equation for the decrease in the concentration of ABA, which is also equal to the rate of formation of acetic acid, is given by

$$\frac{dx}{dt} = \frac{-d[ABA]}{dt} = k_h[ABA]^2 + k_c[ABA][PET] \qquad (1)$$

while for PET we have

$$\frac{-d[PET]}{dt} = k_c[ABA][PET] \qquad (2)$$

Dividing eq 1 by (2) so as to eliminate time results in the following functional relation between [ABA] and [PET]

$$\frac{d[ABA]}{d[PET]} = \frac{k_h[ABA]}{k_c[PET]} + 1 \qquad P(v) = \frac{-k_h}{k_c[PET]}$$

$$Q(v) = 1 \qquad (3)$$

The reactivity ratio k_r can be given as $k_r = k_h/k_c$.

Thus, eq 3 reduces to the well-known form

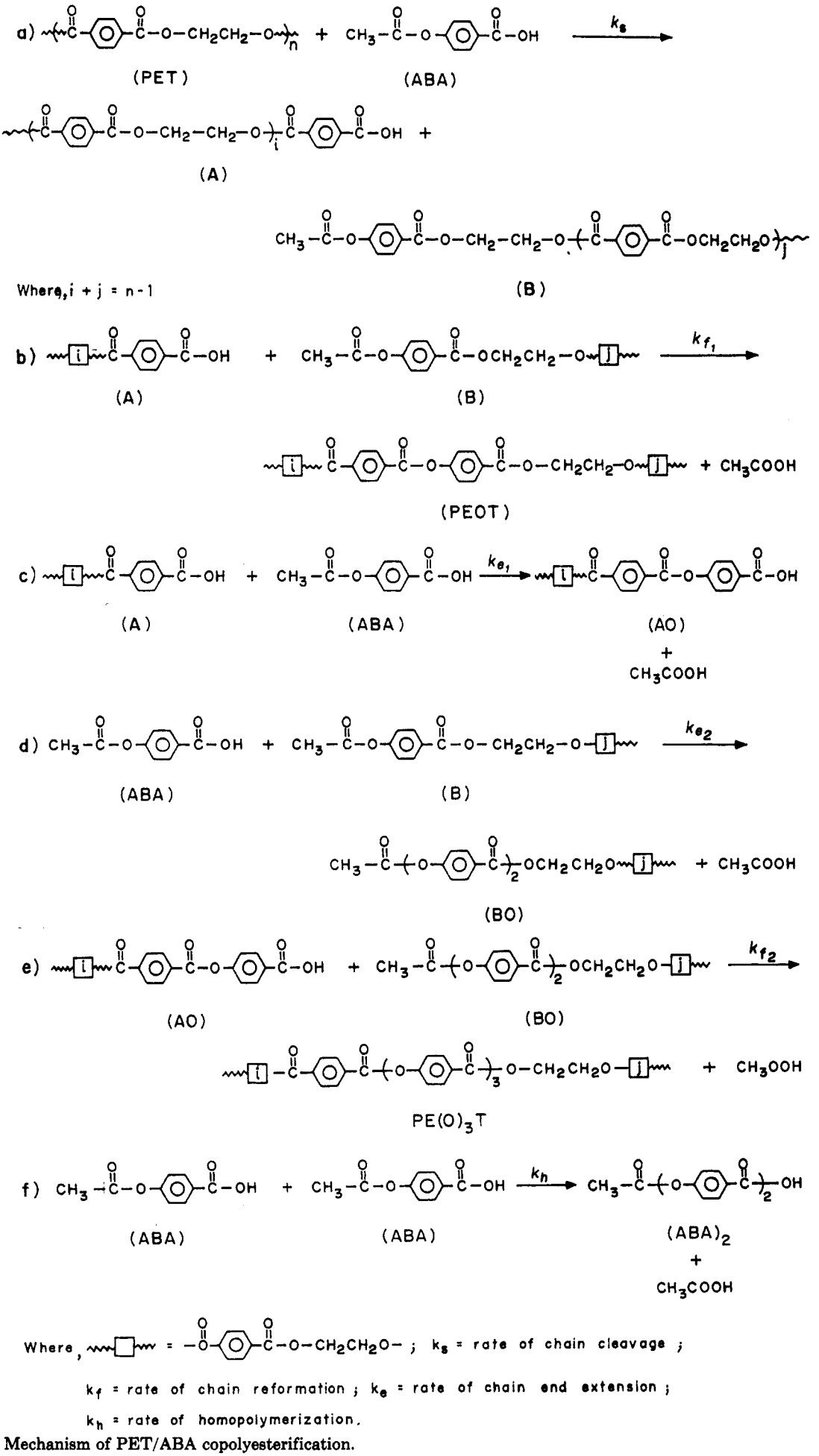

Figure 1. Mechanism of PET/ABA copolyesterification.

$$\frac{du}{dv} + P(v)u = Q(v) \tag{4a}$$

whose solution is represented by

$$ue^{\int P\,dv} = \int Qe^{\int P\,dv} + \text{constant} \tag{4b}$$

Performing the above outlined manipulations, we get

$$[\text{ABA}][\text{PET}]^{-k_r} = \frac{[\text{PET}]^{(1-k_r)}}{(1-k_r)} + \text{constant} \tag{5}$$

which can be rearranged as

$$[\text{ABA}] = \frac{[\text{PET}]}{(1-k_r)} + \text{constant}[\text{PET}]^{k_r} \tag{6}$$

At time $t = 0$, $[\text{ABA}]_0 = a$ and $[\text{PET}]_0 = b$; where a and b are initial concentrations of monomer ABA and PET repeat units (without an ABA unit insertion). This fixes the value of the constant as

$$\text{constant} = \left\{a - \frac{b}{(1-k_r)}\right\}b^{-k_r} \tag{7}$$

Defining

$$\frac{1}{(1-k_r)} = f_1 \qquad \text{constant} = f_2$$

$$[\text{ABA}] = f_1[\text{PET}] + f_2[\text{PET}]^{k_r} \tag{8}$$

Substituting the value of ABA from eq 8 into eq 2 yields

$$\frac{-d[\text{PET}]}{dt} = k_c\{f_1[\text{PET}]^2 + f_2[\text{PET}]^{1+k_r}\} \tag{9}$$

After separating the variables and integrating, we have the following relation between y and t,

$$\int_{[\text{PET}]}^{[\text{PET}]_0} \frac{d[\text{PET}]}{\{f_1[\text{PET}]^2 + f_2[\text{PET}]^{1+k_r}\}} = k_c t \tag{10}$$

Since $[\text{PET}] = b - y$ at any time t, eq 10 is not directly useful for application to experimental data as y is not measured. However, since we are only interested in determining the reactivity ratios k_r, we arbitrarily put $k_c = 1$. Then the right hand side (RHS) of eq 10 becomes equal to time. Now we use y as a parameter in the lower integration limit of the left hand side (LHS) of eq 10 till both the LHS and RHS of eq 10 are equal. In other words for every y we get a corresponding t.

For performing the numerical integration of the left hand side of eq 10, we use a fast and efficient sixteen point Gauss–Legendere procedure.[28] Thus, a perfect match can be achieved between y and t.

What is measured is the moles of acetic acid produced, x, and not y. Therefore, what is required is a relation between x and y, which is easily obtained by rearranging eq 8.

$$x = a - [f_1(b-y) + f_2(b-y)^{k_r}] \tag{11}$$

The numerical procedure followed is essentially the following: Using y as a parameter in the LHS of eq 10, eq 10 is integrated till agreement between the LHS and RHS is obtained (i.e. real time t). Once this real time and y are found, it is substituted into eq 11 such that the mean square deviation between experimentally measured acetic acid and the theoretically predicted moles of acetic acid (summed over all the experimental data points) attains a minimum. So, this can be thought of as a least squares procedure to get the best estimates of the reactivity ratio k_r. Figures 2–15 illustrate the comparison of theoretical acetic acid production with experimental measurements (root square mean deviation of the least squares fit is approximately 5%). Figures 2–15 show that second-order kinetics is generally followed both for homopolyesterifi-

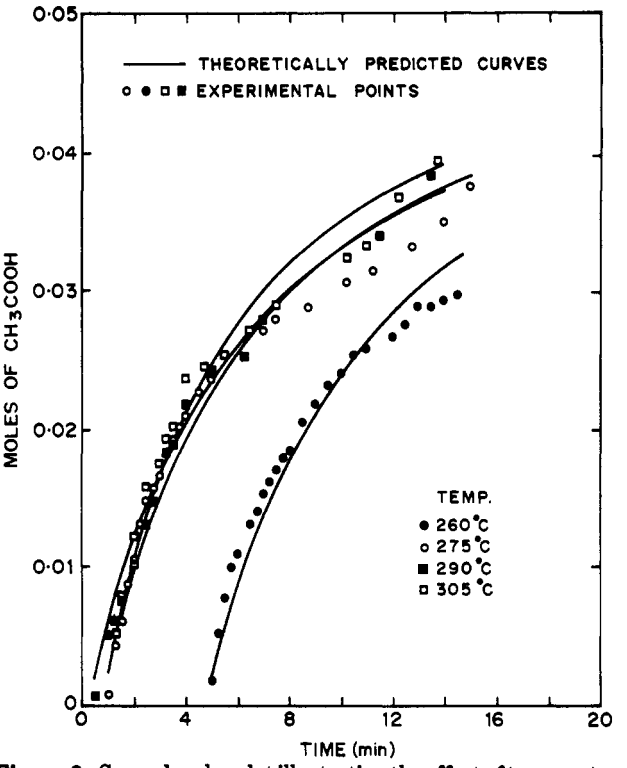

Figure 2. Second-order plot illustrating the effect of temperature for uncatalyzed reactions for the PET/ABA 50 composition.

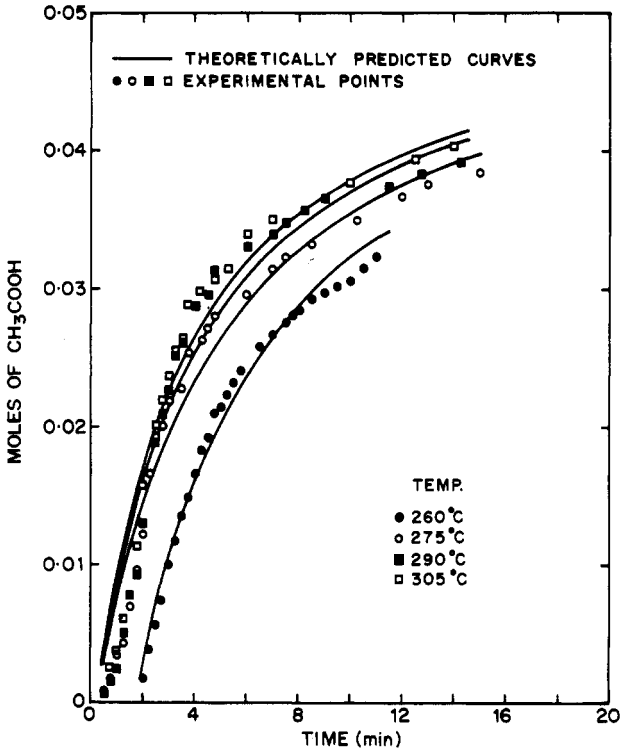

Figure 3. Second-order plot illustrating the effect of temperature for uncatalyzed reactions for the PET/ABA 60 composition.

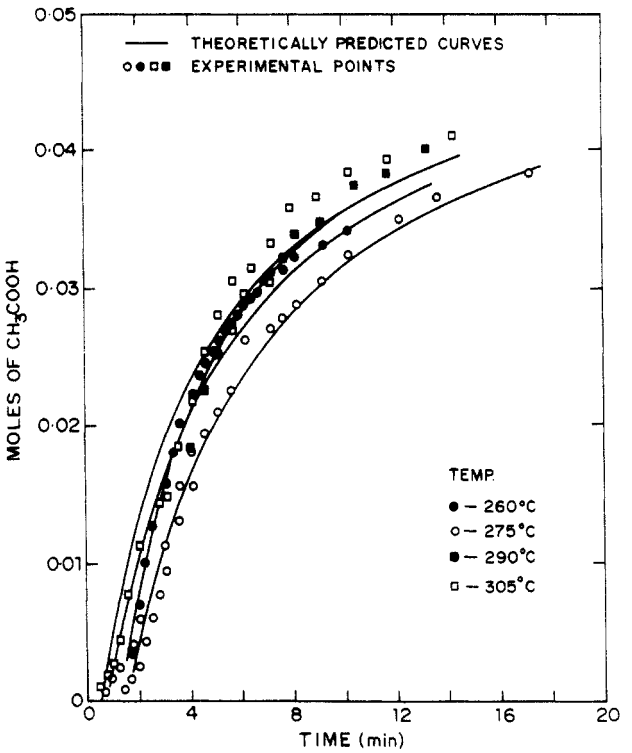

Figure 4. Second-order plot illustrating the effect of temperature for uncatalyzed reactions for the PET/ABA 70 composition.

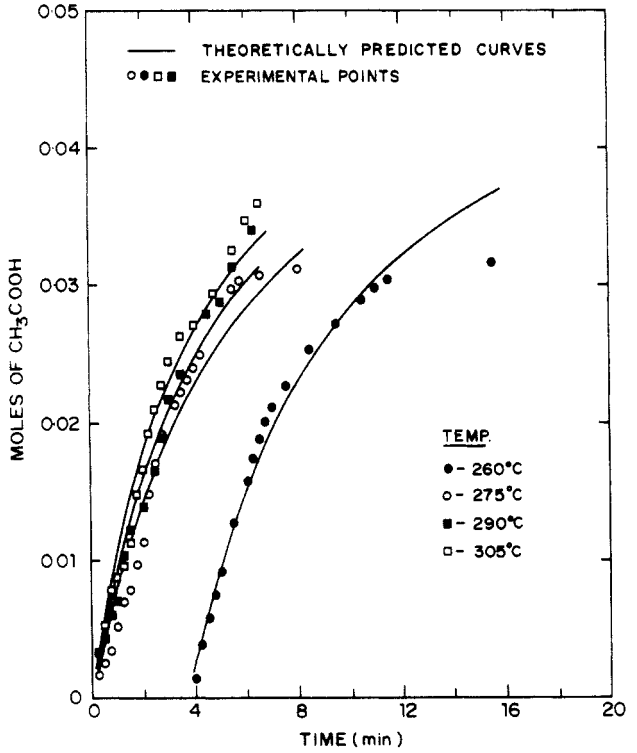

Figure 5. Second-order plot illustrating the effect of temperature for catalyzed reactions for the PET/ABA 50 composition.

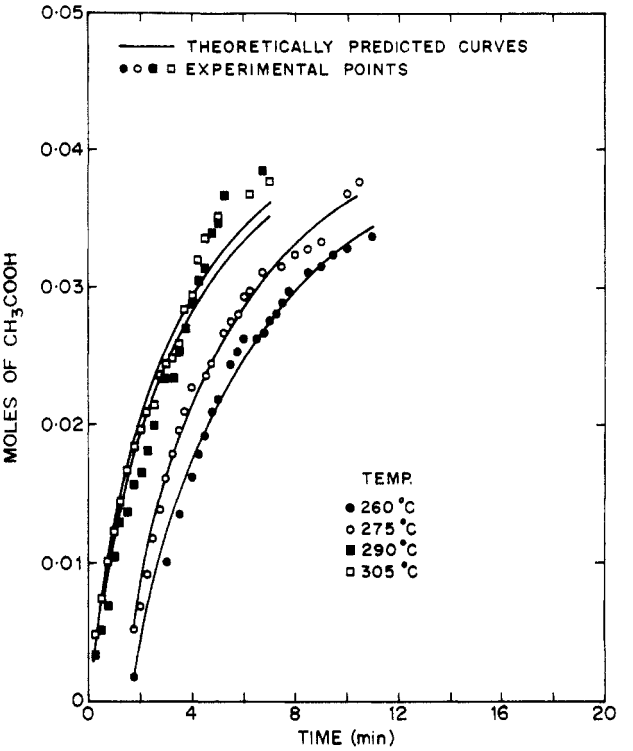

Figure 6. Second-order plot illustrating the effect of temperature for catalyzed reactions for the PET/ABA 60 composition.

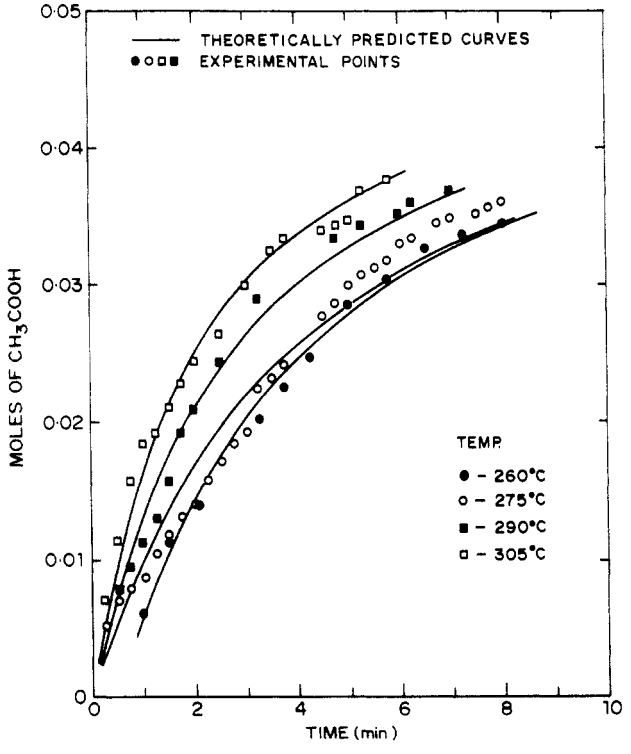

Figure 7. Second-order plot illustrating the effect of temperature for catalyzed reactions for the PET/ABA 70 composition.

cation of ABA as well as in copolyesterification with PET at the three ABA compositions (50, 60, and 70).

A previous study of ABA homopolyesterification has been carried out, and information is available on the kinetics.[24] In that study, one distinguishing feature was observance of breaks in the kinetic plots, indicating the precipitation of oligomers with $\overline{DP} \geq 5$. In the present kinetic analysis, since there are two competing reactions, $1/(1-p)$ cannot be plotted against time to determine the reaction order. However, if there is a significant oligomer precipitation then a priori one would expect two kinetic stages and consequently breaks in the rate (slope) of acetic acid production curves, provided the reactivity ratios favor the homopolyesterification selectively. Since breaks are not observed in the kinetic analysis for most of the runs, it can be concluded that in all probability, oligomer precipitation (arising out of homopolyesterification of 4-acetoxybenzoic acid) does not occur to a significant degree. However, some plots (Figures 16 and 17) suggest a systematic deviation from the single stage kinetics and therefore a two stage kinetic model is warranted. An

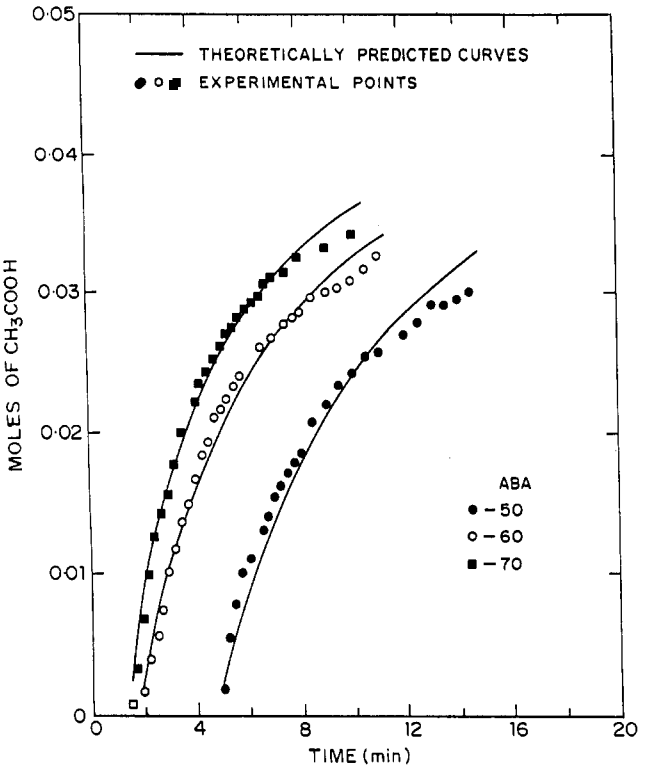

Figure 8. Second-order plot illustrating the effect of composition for uncatalyzed reactions at 260 °C.

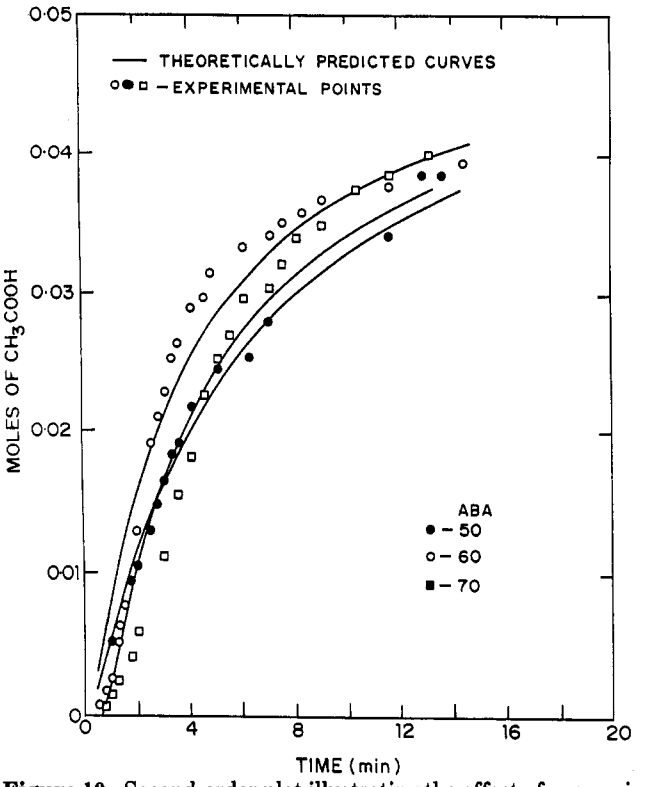

Figure 10. Second-order plot illustrating the effect of composition for uncatalyzed reactions at 290 °C.

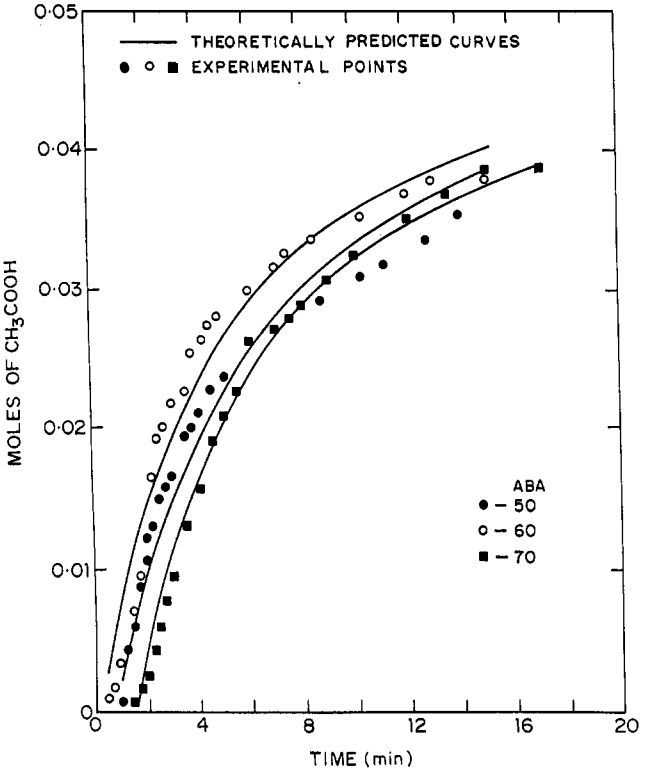

Figure 9. Second-order plot illustrating the effect of composition for uncatalyzed reactions at 275 °C.

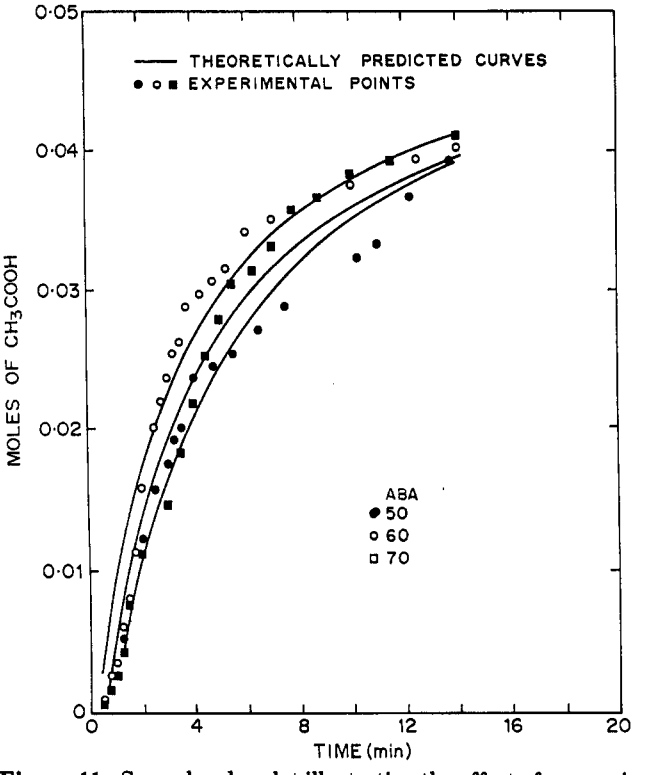

Figure 11. Second-order plot illustrating the effect of composition for uncatalyzed reactions at 305 °C.

attempt is made to employ this strategy with the objective of improving the kinetic treatment of those sets of data points which show a misfit to the single stage model.

The foregoing discussion showed that the single stage model is adequate for most of the runs. Homopolymerization of ABA had been carried out earlier and the rate constant k_h was determined.[24] The k_h we have determined in the present study ought to match the k_h established earlier, since here homopolyesterification occurs in parellel with copolyesterification.

A reference to Table 1 reveals that this is clearly the case. The kinetic constants k_h determined in this study agreed within 10% with those predicted in the previous study.[24] It is also surprising that the kinetic constants for the ABA homopolyesterification reaction, as reflected in the reactivity ratios, remain unaltered even though competing reactions occur between PET blocks and oxybenzoate blocks and also a possibility of change in the

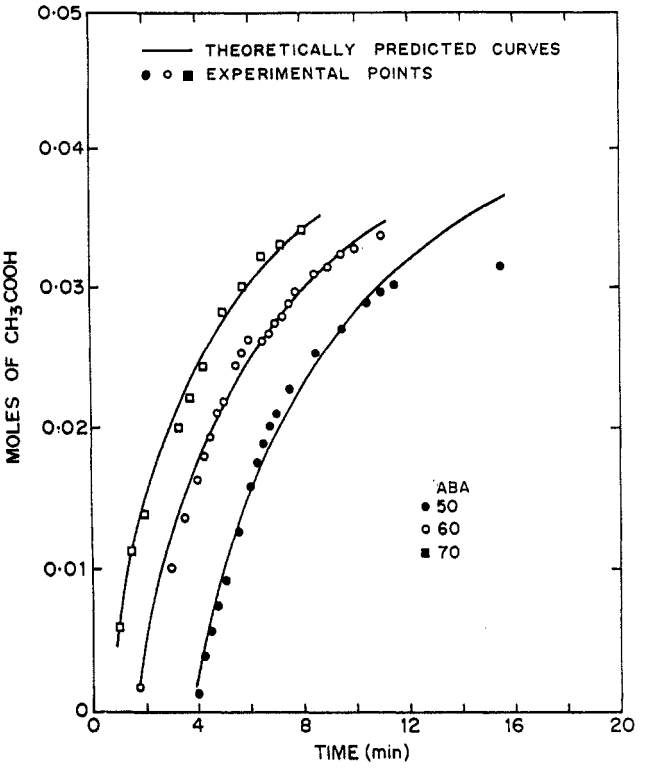

Figure 12. Second-order plot illustrating the effect of composition for catalyzed reactions at 260 °C.

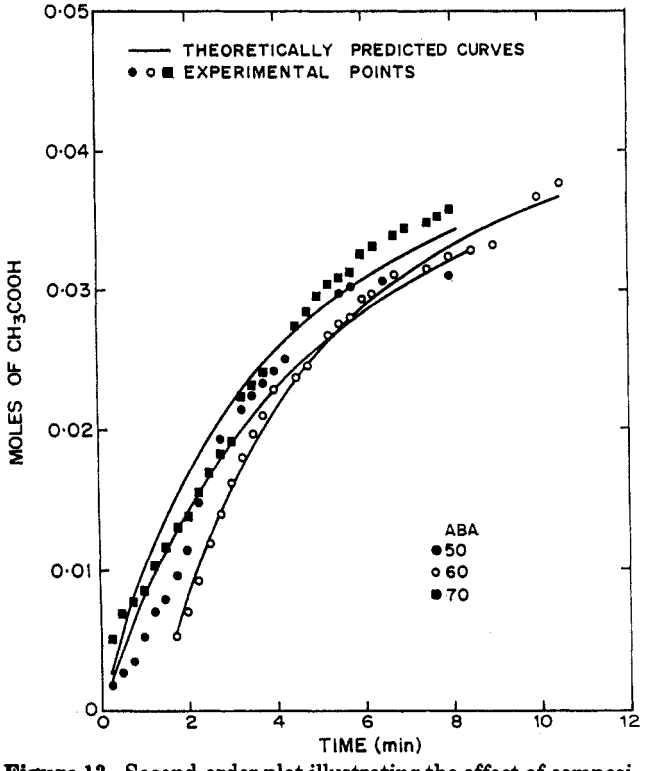

Figure 13. Second-order plot illustrating the effect of composition for catalyzed reactions at 275 °C.

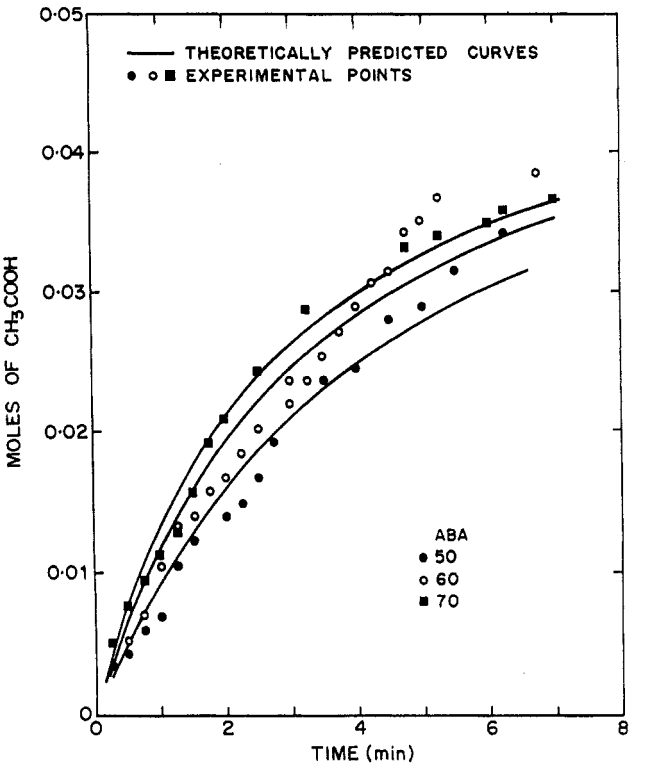

Figure 14. Second-order plot illustrating the effect of composition for catalyzed reactions at 290 °C.

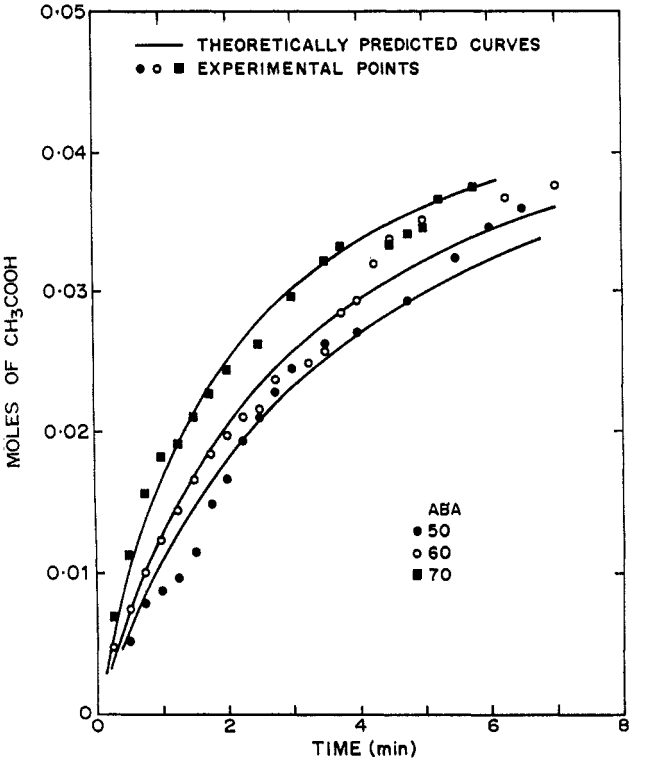

Figure 15. Second-order plot illustrating the effect of composition for catalyzed reactions at 305 °C.

viscosity of the medium exists due to the thermotropic character of the PET/ABA copolyester.

A reference to Table 2 shows that the actual reactivity ratios at a given temperature depend on the composition. It is difficult to precisely define concentration units for a two component system in the melt on a volume basis, when the actual volume of the melt, as a function of conversion, is unknown. However, we get reactivity ratios which are fairly independent of the composition if the reactivity ratios are corrected for the difference in composition by multiplying with the ratio of initial PET to ABA concentration ($k_r^* = k_r[PET]_0/[ABA]_0$). This is necessary because it is more convenient to work with DPN (which in turn is a function of fractional conversion) rather than absolute concentrations while estimating the kinetic constants.

The Arrhenius plots would be further support for such a procedure. The plots should be parallel with identical slopes and differing intercepts. On the other hand, if

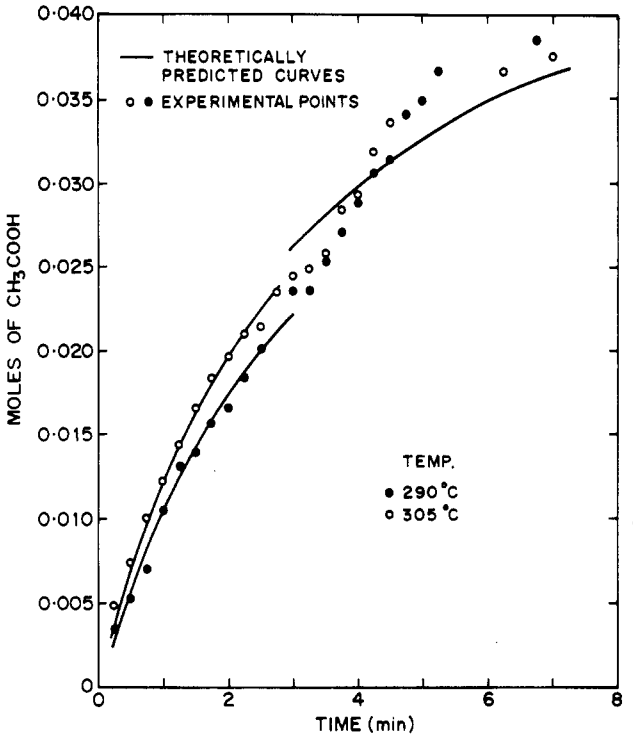

Figure 16. Second-order plot illustrating breaks for PET/ABA 60 catalyzed reactions at temperatures of 290 and 305 °C.

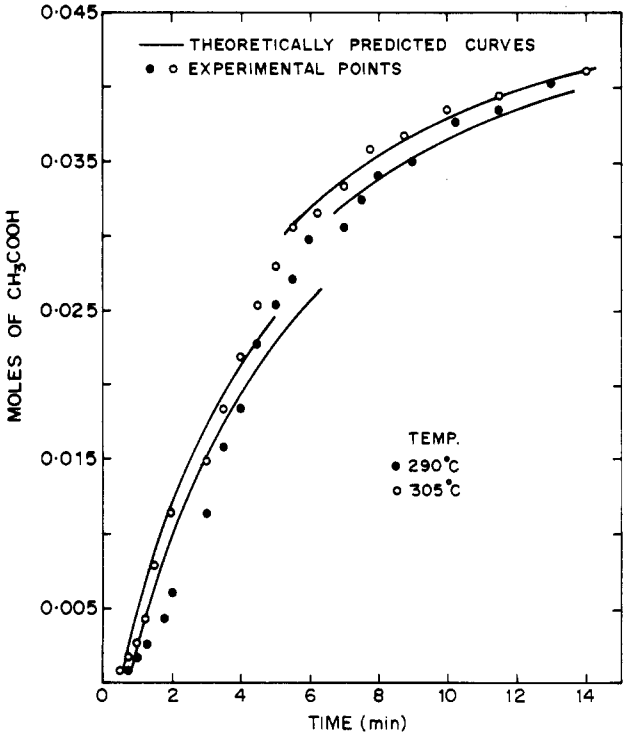

Figure 17. Second-order plot illustrating breaks for PET/ABA 70 catalyzed reactions at temperatures of 290 and 305 °C.

correction is made for composition, the plots should merge into one within experimental error.

The data can be classified into two different types: (i) those emanating from variance in temperature, as presented in Figures 2–7, and (ii) those obtained at constant temperature as composition is varied, as represented in Figures 8–15. These data can be broken into those obtained for catalyzed and uncatalyzed runs. An induction period is present for both uncatalyzed and catalyzed runs. The induction time decreases with increases in (i) reaction temperature and (ii) oxybenzoate mole ratio (content). This is because the homopolyesterification does not reveal

Table 1. Rate Constants from Second-Order Plots of PET/ABA 50, PET/ABA 60, and PET/ABA 70 for Uncatalyzed and Catalyzed Reactions[a]

composition	temp	k_h^{uncat}	k_h^{cat}	k_c^{uncat}	k_c^{cat}	EOA^{uncat}	EOA^{cat}
ABA 100	260	0.0252	0.0332				
	275	0.0409	0.0507			18.63 ● 2	16.3 ± 0.6
	290	0.0645	0.0756				
	305	0.0995	0.1105				
ABA 50	260			0.0116	0.0125		
	275			0.0158	0.0177	14.00 ± 2	9.4 ± 1
	290			0.0276	0.0214		
	305			0.0302	0.0252		
ABA 60	260			0.0076	0.0095	12.85 ± 1	8.9 ± 1
	275			0.0108	0.0110		
	290			0.0142	0.0137		
	305			0.0200	0.0182		
ABA 70	260			0.0050	0.0068	19.3 ● 3	6.9 ± 3
	275			0.0120	0.0111		
	290			0.0162	0.0113		
	305			0.0219	0.0118		

[a] k_h represents rate constants (L mol^{-1} s^{-1}) for poly(4-oxybenzoate); k_c represents rate constants (L mol^{-1} s^{-1}) for poly(ethylene terephthalate-co-oxybenzoate). Abbreviations: temp = reaction temperature in degrees centigrade; uncat = uncatalyzed reactions; cat = catalyzed reactions; EOA cat = energy of activation (kcal/mol). ABA 100 represents values reported from an earlier paper.[24]

Table 2. Experimental k_r and k_{r^*} Uncorrected and Corrected Values for Composition[a]

ABA composition	temp, °C	k_r^{uncat}	$k_{r^*}^{uncat}$	k_r^{cat}	$k_{r^*}^{cat}$
ABA 50	260	2.18		2.66	
	275	2.58		2.86	
	290	2.34		3.54	
	305	3.3		4.38	
ABA 60	260	3.3	2.2	3.5	2.33
	275	3.78	2.52	4.62	3.08
	290	4.54	3.02	5.5	3.66
	305	4.98	3.32	6.06	4.04
ABA 70	260	4.98	2.13	4.86	2.08
	270	3.46	1.48	4.58	1.96
	290	3.98	1.7	6.7	2.87
	305	4.54	1.94	9.34	4.00

[a] k_r represents the uncorrected rate constant ratio; k_{r^*} represents the corrected rate constant ratio. Blank entries mean that concentrations are equal and therefore no correction is required.

an appreciable induction period, especially at higher reaction temperatures.

A common feature in all these plots is the general adherence to second-order kinetics, which is fairly obeyed.

One significant experimental point to note is that the maximum temperature employed in copolyesterification experiments was 305 °C. This is approximately 50 deg lower than the maximum temperature employed in the homopolyesterification study of oxybenzoate discussed in our earlier work.[24] The ratio k_{h_1}:k_{h_2} of rate constants k_{h_1} and k_{h_2}, observed for stages 1 and 2 in homopolyesterification of ABA, were evaluated using the preexponential factors and activation energies. It may be recalled that in the present context k_{h_1} and k_{h_2} denote rate constants for hompolyesterification of ABA before and after precipitation, respectively. One would not a priori expect breaks in the kinetic plots at 305 °C even if homopolyesterification was the only reaction occurring. However, breaks are possible at 350 °C where the maximum ratio of rate constants in the two stage kinetics analysis (using 0.1 mol % DBTO as catalyst) is 8.35.[24]

Indeed, replotting the data at 305 °C with a two stage kinetic model gave kinetic ratios $(k_{h_2}/k_{c_2})/(k_{h_1}/k_{c_1})$ which are approximately of the order of 1.5. This shows that there is a marginal advantage in emplying a two stage kinetic model. In other words reactivity ratios (before and after precipitation) of the two stage model differ from

each other only slightly. Figures 16 and 17 clearly illustrate this point. The break is barely perceptible in Figure 17 whereas in Figure 16 it is difficult to note any real break. Reference to the reactivity ratios of Table 2 clearly shows that the variation in reactivity ratios is much less and is about 15% lower than that based on theoretical prediction.

Temperature Variation of the Kinetic Constant for Copolyesterification. The variability of the reactivity ratio is well in accordance with our theoretical expectation and reflects the trend shown by k_h, the kinetic constant for homopolyesterification. We can safely assume these values determined earlier to be exact and use them to get information on k_r, the absolute reactivity ratios for copolyesterification. The kinetic constants, corrected for the compositional variation, should show an Arrhenius type relationship with temperature. This statement holds well if the oxybenzoate blocks are incorporated in a random fashion in the copolyester with PET.[29] On the other hand, if there is a significant blocking of the ABA monomer sequences we would expect systematic deviation from second-order kinetics, especially at higher concentration levels of ABA. Again, the fact that this is not observed gives indirect support for the random block structure.

Figures 18 and 19 describe the Arrhenius plot, which is fairly well obeyed. The preexponential factors and the activation energy strongly suggest that the reaction may be diffusion controlled (random Brownian diffusion). Assuming the Stokes–Einstein equation to be valid for computing the diffusivity, one can make an order of magnitude calculation for the overall rates under the diffusion controlled conditions. However, we bear in mind that actual viscosities, which are only truly meaningful, cannot be measured experimentally and this is the serious limitation of the analysis. Therefore, we omit the details. In general, we could not find quantitative agreement of the rate constants with a Stokes–Einstein model.

A More Complex Kinetic Model. The major reactions depicted in Figure 1 can be represented by eqs V–X.

$$\mathrm{PET} + \mathrm{ABA} \xrightarrow{k_s} \mathrm{A} + \mathrm{B} \qquad \text{(V)}$$

$$\mathrm{A} + \mathrm{B} \xrightarrow{k_{f_1}} \mathrm{PEOT} + \mathrm{CH_3COOH} \qquad \text{(VI)}$$

$$\mathrm{A} + \mathrm{ABA} \xrightarrow{k_{e_1}} \mathrm{AO} + \mathrm{CH_3COOH} \qquad \text{(VII)}$$

$$\mathrm{B} + \mathrm{ABA} \xrightarrow{k_{e_2}} \mathrm{BO} + \mathrm{CH_3COOH} \qquad \text{(VIII)}$$

$$\mathrm{AO} + \mathrm{BO} \xrightarrow{k_{f_2}} \mathrm{PE(O)_3T} + \mathrm{CH_3COOH} \qquad \text{(IX)}$$

$$\mathrm{ABA} + \mathrm{ABA} \xrightarrow{k_h} (\mathrm{ABA})_2 + \mathrm{CH_3COOH} \qquad \text{(X)}$$

k_s, k_f, k_e, and k_h respectively denote the kinetic constants for PET chain scission, PET chain re-formation with insertion of an oxybenzoate unit, extension of the PET chain segment (A and B), and homopolyesterification.

At steady state, the rate of acetic acid production in terms of PET and 4-acetoxybenzoic acid concentrations is given by eq 12 (see Appendix A). When this equation

$$\frac{dx}{dt} = 3k_s[\mathrm{PET}][\mathrm{ABA}] + k_h[\mathrm{ABA}]^2 - \left(\frac{2k_{f_1}k_{e_1}}{k_{e_2}}\right)[\mathrm{A}]^2 \qquad (12)$$

(12) is expressed in terms of relative rates with respect to

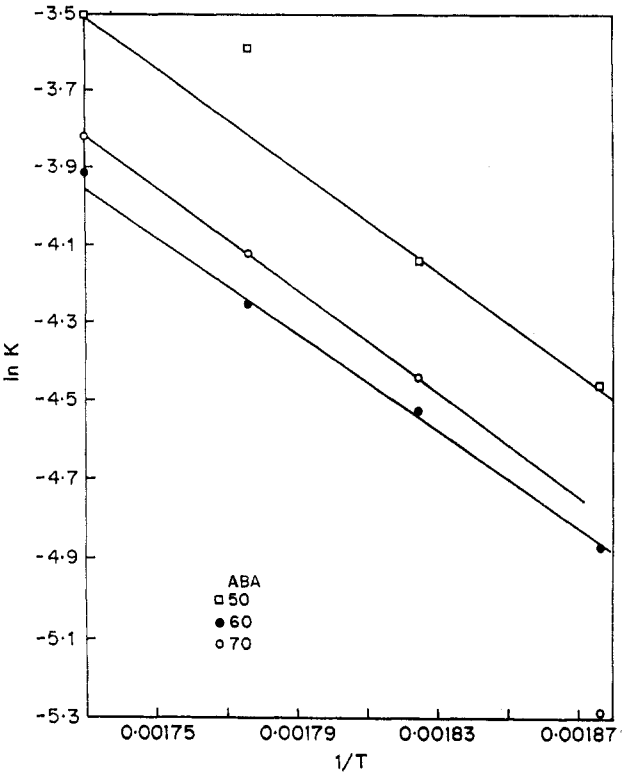

Figure 18. Arrhenius plot for uncatalyzed reactions.

$3k_s$ (this is equal to k_c of the simple kinetic model (eq 1)], we then get

$$\frac{dx}{dt} = [\mathrm{PET}][\mathrm{ABA}] + k'_r[\mathrm{ABA}]^2 - \lambda[\mathrm{A}]^2 \qquad (13)$$

where

$$\lambda = \frac{2k_{f_1}k_{e_1}}{3k_sk_{e_2}} \qquad k'_r = \frac{k_h}{3k_s}$$

By comparison with the rate equations of the previous section (eq 1), the rate of production of acetic acid is modified by the third correction term in eq 13, when we employ the more elaborate model.

If the steady state assumption is not valid, i.e. concentrations [A], [B], [AO], and [BO] are not negligible, then the rate of acetic acid generation is given by the algebraic sum of all rate equations producing acetic acid (eqs VI–X)

$$\frac{dx}{dt} = k_{f_1}[\mathrm{A}][\mathrm{B}] + k_{e_1}[\mathrm{A}][\mathrm{ABA}] + k_{e_2}[\mathrm{B}][\mathrm{ABA}] + k_{f_2}[\mathrm{AO}][\mathrm{BO}] + k_h[\mathrm{ABA}][\mathrm{ABA}] \qquad (14)$$

There are six rate constants, k_s, k_{f_1}, k_{e_1}, k_{e_2}, k_{f_2}, and k_h, associated with eqs V–X. The measured variable is only one, namely the production of acetic acid. Thus, the six parameter model needs to be truncated to be suitable for a kinetic evaluation of the process. Such a truncation into a three parameter model is feasible by validating an equivalence between the rate constants of reactions of segment A with segment B and segment A with 4-acetoxybenzoic acid, assuming Flory's principle of equal reactivity.[30] These are the two reactions of a carboxylic acid terminated PET segment with (a) a PET segment having an acetoxy end group and (b) an acetoxy group of 4-ABA, respectively. Then, $k_{f_1} = k_{e_1} = k_t$. Similarly, the rate constants associated with the reactions of (i) segment B with 4-ABA, (ii) segment AO with segment BO, and (iii)

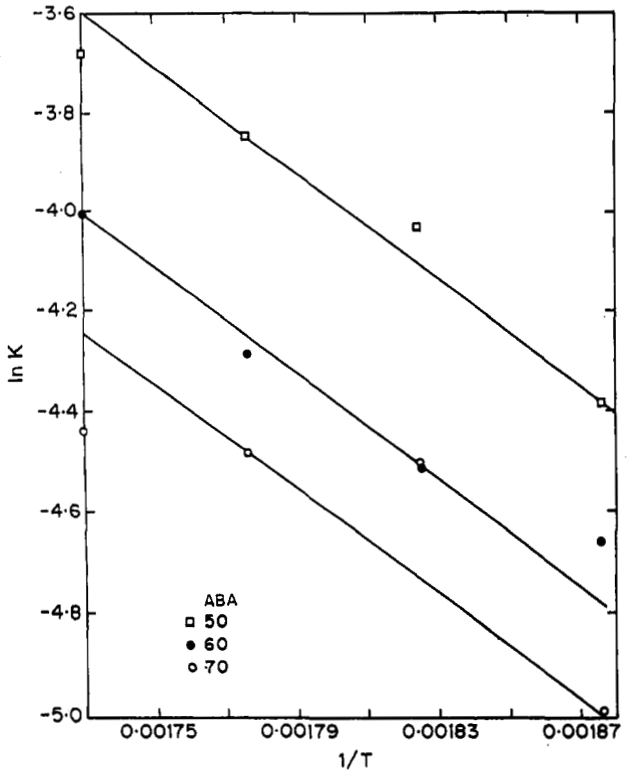

Figure 19. Arrhenius plot for catalyzed reactions.

homopolyesterification of 4-ABA could be deemed equivalent. Then, $k_{f_2} = k_{e_2} = k_h = k_\alpha$. On incorporation of the above equivalence in eq 14, we get

$$\frac{dx}{dt} = k_t[A]([B] + [ABA]) + k_\alpha[ABA]([B] + [ABA]) + k_\alpha[BO][AO]$$

$$\frac{dx}{dt} = (([B] + [ABA])(k_t[A] + k_\alpha[ABA])) + k_\alpha[BO][AO] \quad (15)$$

The concentrations [A], [B], [AO], and [BO] are determined by the following expressions

$$\frac{d[A]}{dt} = k_s[ABA][PET] - k_t[A][B] - k_t[ABA][A] \quad (16)$$

$$\frac{d[B]}{dt} = k_s[ABA][PET] - k_t[A][B] - k_\alpha[ABA][B] \quad (17)$$

$$\frac{d[AO]}{dt} = k_t[ABA][A] - k_\alpha[AO][BO] \quad (18)$$

$$\frac{d[BO]}{dt} = k_\alpha[ABA][B] - k_\alpha[AO][BO] \quad (19)$$

As a result of PET chain cleavage segment A and segment B are formed. Therefore, the concentrations [A], [B], [AO], and [BO] are dependent on the rate of PET chain cleavage k_s. The rate constant of chain cleavage k_s along with the rates k_α and k_t forms a three parameter model. This model is used for least squares fitting of experimental data at the two extreme cases, viz. (a) the uncatalyzed reaction at 275 °C for the PET:ABA (50:50) copolyester and (b) the catalyzed reaction at 305 °C for the PET:ABA (70:30) copolyester, as shown in Figure 20 using the Runge–Kutta procedure and compared with the fitting done using the two parameter model discussed in the previous section (eq 1). The Runge–Kutta procedure is used to integrate

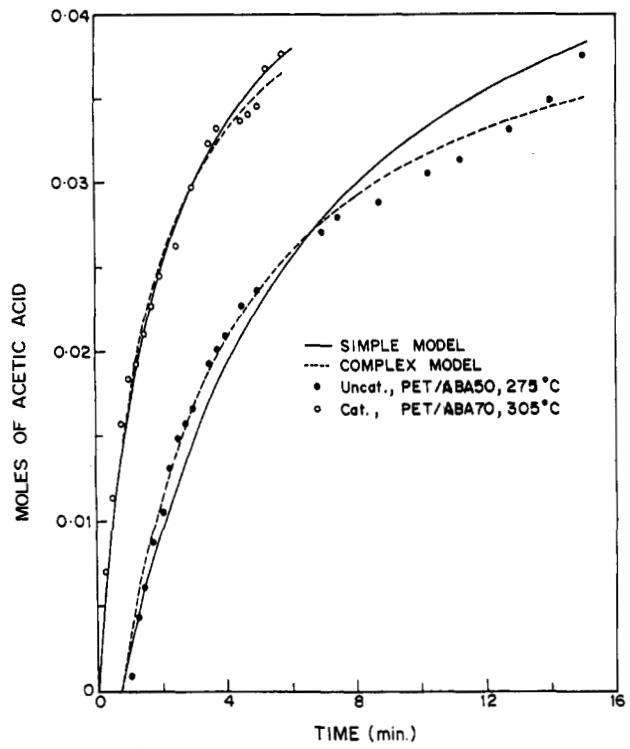

Figure 20. Plot illustrating the comparison between simple and complex kinetic models.

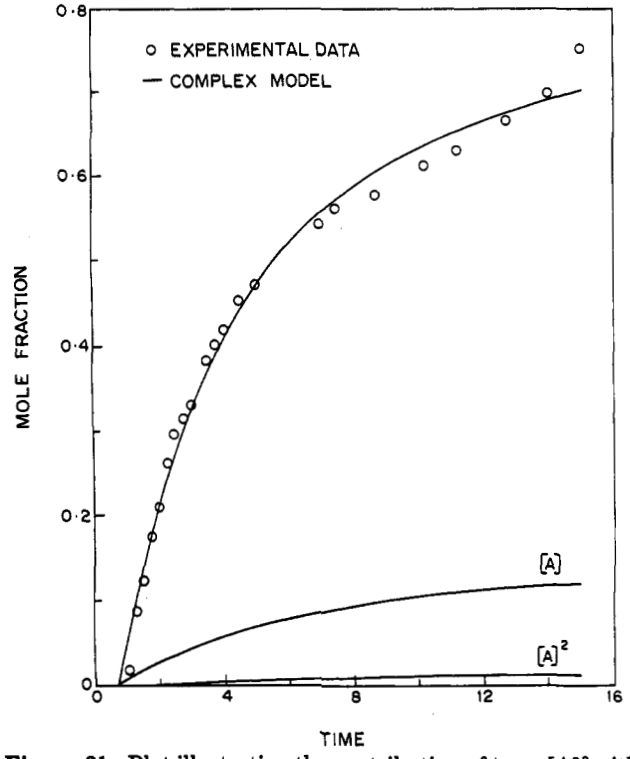

Figure 21. Plot illustrating the contribution of term $[A]^2$ with respect to the overall production of acetic acid for the PET/ABA 50 uncatalyzed reaction at 275 °C.

the ordinary differential eq 15–19. The rate constants k_s, k_α, and k_t are varied till least squares fitting of experimental data is obtained. The fit improved only marginally with this complex model. This also confirms the applicability of the simple model proposed in the previous section. The concentration [A] and $[A]^2$ obtained from the above procedure for the uncatalyzed reaction of PET:ABA (50:50) at 275 °C, is shown in Figure 21. It is clear from the figure that the contribution of the correction term is negligible as far as the overall acetic acid production is concerned. If this term is eliminated from eq 13, we get

$$\frac{dx}{dt} = [PET][ABA] + k'_r[ABA]^2 \quad (20)$$

where $k'_r = k_h/3k_s$. This expression is identical with the model proposed in the section on simple kinetics.

$$\frac{dx}{dt} = [PET][ABA] + k_r[ABA]^2$$

where $k_r = k_h/k_c$.

Characterization

All copolyesters synthesized in this study, PET/20 ABA to PET/70 ABA were soluble in the phenol–tetrachloroethane mixture (60:40 v/v) at a concentration of 0.5 gm/dL. It may be recalled that the transesterifications were stopped once the evolution of acetic acid ceased to occur under atmospheric pressure. The copolyesters were indeed oligomers, as seen from the low inherent viscosities. Inherent viscosities (IV) of PET/20 ABA, PET/30 ABA, and PET/40 ABA were in the range 0.15–0.20. The PET/50 ABA, PET/60 ABA, and PET/70 ABA copolyesters had inherent viscosities in the range 0.2–0.25.

The samples were heated at 10 °C/min from room temperature to 325 °C, the upper limit of the microscope. Depolarization of light was observed for all samples (except PET/20 ABA and PET/30 ABA). The microscopic observations also revealed the absence of nonmelting poly(4-oxybenzoate) in the copolyesters, which would be seen as nonmelting anisotropic regions.

DSC thermograms of the second heating cycle (heating rate, 10 °C/min) for the samples ABA (30–70) synthesized in the present study are shown in Figure 22. The first cycle consisted of heating the sample above the liquid crystalline transition temperature at 20 °C/min and cooling to 50 °C at the rate of 100 °C/min. The thermodynamic parameters pertinent to the first- and second-order transitions are tabulated in Table 3.

The entities present in the copolyester may be represented globally by the following structure. Here, a and b

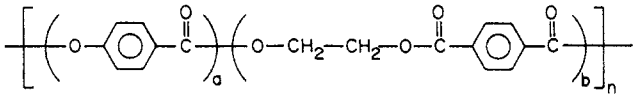

are the mole percent of oxybenzoate and PET units along the chain. At 50 mol % of oxybenzoate ($a = b$), the structures would resemble a rigid rod–flexible spacer type thermotropic system comprising a diad mesogen with carboxylic groups coupled to 1,2-ethanediol. At a lower (<50) mole percent of oxybenzoate, the globally averaged mesogen would continue to be the diad. Here, the flexible spacer would have to encompass terephthaloyl and hence ethylene–terephthalate units. This would be crystalline. At a sufficiently low (<30) mole percent of oxybenzoate the mesogen is sufficiently diluted at the expense of increasing the concentration of crystalline ethylene terephthalate moieties and the thermotropic character is known to disappear. Above 50 mol % of oxybenzoate in the copolyester, the averaged mesogen length would increase while the flexible spacer will remain unchanged and comprise dimethylene units arising from 1,2-ethanediol. At a sufficiently high (>60) mole percent of oxybenzoate, the averaged mesogen formed is nonmelting and thermotropic character disappears yet again. In randomized incorporation of oxy benzoate along the PET chain the structure formed would deviate appreciably from the globally averaged one. The mesogens formed along a copolyester chain would have a very wide distribution of

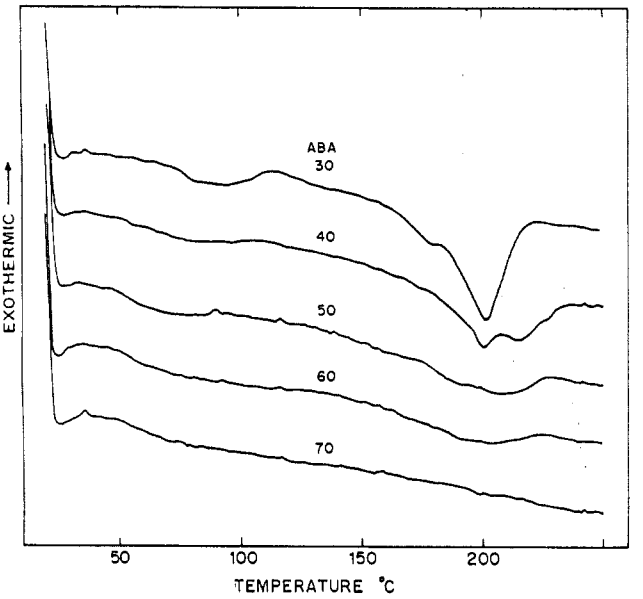

Figure 22. DSC endotherms of PET/ABA systems for the samples synthesized at 305 °C (second heating cycle).

Table 3. Transition Temperatures and Thermodynamic Data for Uncatalyzed Reactions for the Second Heating Cycle[a]

sample code	T_g, °C	T_c, °C	T_m, °C	ΔH_m, kcal/mol	ΔS_m
PET[b]	80	153			
PET/20 ABA	76	110			
PET/30 ABA	76	117	200	1.90	4.0
PET/40 ABA	63		201	1.10	2.2
PET/50 ABA	56		206	0.25	0.53
PET/60 ABA	57		199	0.15	0.32
PET/70 ABA	62				

[a] Conditions: reaction temperature, 305 °C; reaction time, 1.0 h; heating rate, 10 °C/min. Abbreviations: T_g = glass transition temperature; T_c = cold crystallization peak temperature; T_m = crystal to liquid crystal melting peak temperature; ΔH_m represents enthalpy values for crystal to liquid crystal melting; ΔS_m represents entropy values for crystal to liquid crystal melting. [b] The PET isotropic melting temperature is 256 °C.

aspect ratios. Oxybenzoate oligomer is nonmelting above a degree of polymerization 6. Transesterification of mesogenic acetate with aliphatic dicarboxylic acid in the temperature range 200–280 °C has been shown to randomize the repeating units along the polymer chain. This generates blocks with differing sequence lengths of oxybenzoate determinable by ^{13}C NMR.[29,31] Such polymers form biphasic melts.[31] In the present system, thermotropic character ought to be observable till a sequence length of 6 ABA units. This would correspond to 85.7 mol % of ABA units in the copolyester. However, thermotropicity disappears above 60 mol % of ABA in the copolyester. This points to the formation of nonmelting (>6) blocks of ABA and thereby randomization of structural entities along the chain. It has been shown, however, that there exists a preference factor for ABA insertion which deviates from complete randomization by 1.3.[29] The exact structure in ordered systems on the other hand would closely resemble the globally averaged one. Here, the averaged aspect ratio of the mesogens formed would be akin to those actually present along the copolyester chain. These systems would continue to display thermotropic character at a higher mole percent of oxybenzoate units along the chain as compared to a random blocked structure. DSC thermograms would therefore qualitatively differ depending on the microstructure of the copolyester.

Before the compositions of the copolyesters are speculated upon, it is to be borne in mind that the reactivity

ratios (i.e. the ratio of kinetic constants k_r) deviate appreciably from unity in most of the cases. If k_r was equal to unity, then the composition of the copolyester would have mirrored the initial stoichiometry. However, in the absence of direct experimental data on the composition of the copolyester, the following discussion is only tentative as far as the compositions of the copolyesters are concerned. The kinetic analysis clearly shows that even though there may be uncertainty in the composition of the copolyester, there cannot be blocking of the oxybenzoate units with block size ≥5. In other words, the kinetic analysis excludes blocking and suggests indirectly that a random block structure of PET/oxybenzoate moieties is formed. Polarizing microscopic observations did not reveal evidence of any nonmeltable fractions. (Obviously, even if homopolyesters of ABA are present, the DP has to be ≤5. Also, the sequence length of oxybenzoate in the PET/ABA copolyester must be ≤5 to retain thermotropic character.)

The T_g has a maximum value of 80 °C for PET ($\bar{M}_n$ = 20 000). As we systematically increase the ABA content, the T_g dips and goes through a minimum at 50 mol % of oxybenzoate (56 °C), corresponding to equimolar composition. If the system was to form a totally random copolyester, it is obvious from first principles that the maximum randomization will occur at 50 mol %. This is turn will have the maximum segmental mobility and therefore have a minima in T_g, as is observed experimentally.

An additional feature is the presence of cold crystallization in the thermogram which shows the onset of crystallization stimulated by thermal annealing. We would expect this peak to be present at least for those compositions wherein the mole percent of PET is higher, as shown for the two compositions PET/ABA 20 and 30.

As mentioned earlier, the onset of liquid crystallinity is observable in the system above 30 mol % of ABA. We observe a first-order solid to liquid crystalline endotherm corresponding to this transition. The T_m, ΔH_m, and ΔS_m values for this liquid crystalline transition are presented in Table 3.

The progressively decreasing ΔH_m values for copolyesters synthesized from increasing 4-acetoxybenzoic acid content in the reaction mixture, from 20 to 70 mol %, is an indirect confirmation of the insertion of oxybenzoate units into the PET chain, which decreases the crystallinity of the system. The ΔS_m values are typical of a solid to nematic transition. A typical nematic texture was observed under the polarizing microscope for these (ABA 50, 60, 70) three compositions.

Following the original approach by Flory,[32] we may try to fit a thermodynamic equation (21), which has been

$$\frac{1}{T_m} - \frac{1}{T_m^\circ} = -\frac{R}{\Delta H_{\mu_1}} \ln x_1 \qquad (21)$$

applied to the transformation of a solid to isotropic liquid (where T_m and T_m° are the equilibrium melting temperatures of copolyester and PET respectively, R is the gas constant in energy units, ΔH_{μ_1} is the heat of fusion of PET, and x_1 is the mole fraction of comonomer (PET) in the copolyester). This has been employed by a number of workers[18] for analyzing crystal to liquid crystal transitions.

Although this equation has limited validity in describing the crystal to liquid crystal transition, it gives a reasonable fit to the rather limited experimental data shown in Figure 23. Since neither PET nor poly(4-oxybenzoate) is a thermotropic crystal, it is difficult to relate this experimentally observed ΔH_m to the segmental enthalpy of crystal to liquid crystal transition of either PET or oxybenzoate blocks. Obviously, this ΔH has to be much smaller than the enthalpy of fusion of the PET segment (solid to isotropic melt).

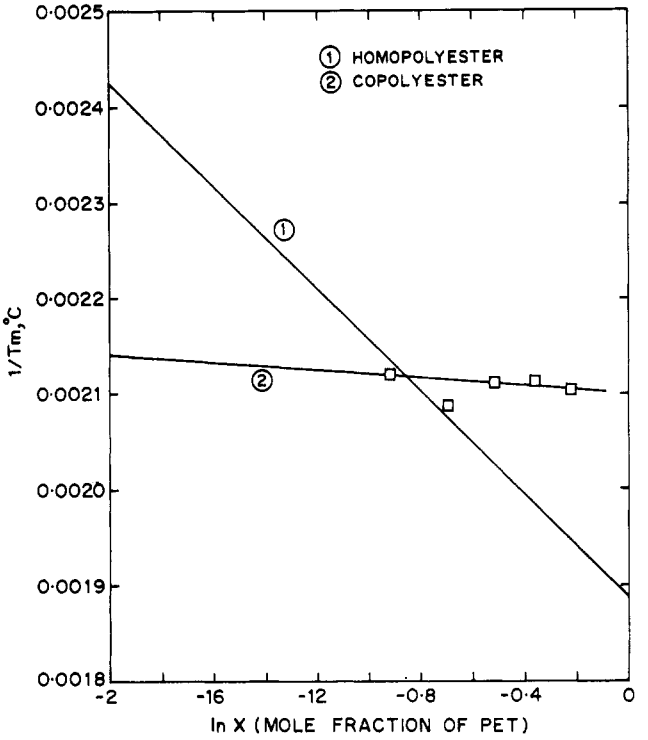

Figure 23. Plot of melting temperature versus mole percent of PET.

Conclusions

The kinetics of melt copolyesterification of PET/50 ABA, PET/60 ABA, and PET/70 ABA has been studied using simple phenomenological models. A parallel second-order reaction scheme adequately represents the kinetics of ABA homopolyesterification and PET/ABA copolyesterification. The kinetics of catalyzed reactions also follow the same reaction order. A kinetic study for ABA homopolyesterification revealed breaks in the second-order plots, mainly arising out of oxybenzoate oligomer precipitation for DP ≥ 5. However, such breaks are not observed when homopolyesterification and copolyesterification take place simultaneously. This clearly implies that oxybenzoate oligomers with DP ≥ 5 are not formed. Kinetically, the rate constants computed here for oxybenzoate homopolyesterification correspond to the first stage of oxybenzoate polyesterification kinetics.

A simple numerical procedure involving the Gauss–Legendre quadrature computes the amount of acetic acid produced, and the reactivity ratios are determined by minimizing the least squares variation between the theoretical and experimental amounts of acetic acid produced.

The copolyesterification kinetics is characterized by the rate constants which are several fold lower than those for ABA polyesterification. The activation energy values for the uncatalyzed and catalyzed reactions are significantly different. The reaction is visualized as occurring quantitatively when an ABA monomer strikes the surface of a random coil of PET which is assumed to be spherical in shape. The distribution of oxybenzoate segments in the

PET surface is supposed to be random, and this adequately gives the observed second-order kinetics.

Unlike in homopolyesterification of 4-acetoxybenzoic acid no compensation effect or predominant influence of entropy of activation was noticed in ABA homopolyesterification occurring during the copolyesterification between PET and 4-acetoxybenzoic acid.

Optical microscopy characterizations of the copolyesters show clearly that the PET/ABA 30–ABA 70 composition range gives rise to a nematic liquid crystal morphology.

Our DSC studies in general support the idea of a random block structure for the copolyester. Meltable copolyesters are obtained at all compositions. An upper limit to the oxybenzoate block (based on DSC observations) would be approximately $\overline{DP} = 5$.

Acknowledgment. The work was supported by funding from the New Fibres and Composites group, Department of Science and Technology, New Delhi. The authors are obliged to Miss B. Gokhale for the experimental help provided during the course of this work.

Appendix A

It is the main aim of this appendix to show that by invoking the steady state approximation for the rate of production of intermediate species A, B, AO, and BO, a simple kinetic picture emerges. The reactions involved are (see text for nomenclature)

$$\mathrm{PET + ABA \xrightarrow{k_s} A + B} \qquad \text{(A-I)}$$

$$\mathrm{A + B \xrightarrow{k_{f_1}} PEOT + CH_3COOH} \qquad \text{(A-II)}$$

$$\mathrm{A + ABA \xrightarrow{k_{e_1}} AO + CH_3COOH} \qquad \text{(A-III)}$$

$$\mathrm{B + ABA \xrightarrow{k_{e_2}} BO + CH_3COOH} \qquad \text{(A-IV)}$$

$$\mathrm{AO + BO \xrightarrow{k_{f_2}} PE(O)_3T + CH_3COOH} \qquad \text{(A-V)}$$

$$\mathrm{ABA + ABA \xrightarrow{k_h} (ABA)_2 + CH_3COOH} \qquad \text{(A-VI)}$$

$$\mathrm{PET + 5ABA + [A] + [B] \rightarrow PEOT + PE(O)_3T + 5CH_3COOH}$$

Assuming simple second-order kinetics for each of the reaction sequences (A-I)–(A-VI), we have the following equations:

$$\frac{d[A]}{dt} = k_s[ABA][PET] - k_{f_1}[A][B] - k_{e_1}[ABA][A] \qquad \text{(A1)}$$

$$\frac{d[B]}{dt} = k_s[ABA][PET] - k_{f_1}[A][B] - k_{e_2}[ABA][B] \qquad \text{(A2)}$$

$$\frac{d[AO]}{dt} = k_{e_1}[ABA][A] - k_{f_2}[AO][BO] \qquad \text{(A3)}$$

$$\frac{d[BO]}{dt} = k_{e_2}[ABA][B] - k_{f_2}[AO][BO] \qquad \text{(A4)}$$

By steady state approximation

$$\frac{d[A]}{dt} = \frac{d[B]}{dt} = \frac{d[AO]}{dt} = \frac{d[BO]}{dt} = 0 \qquad \text{(A5)}$$

Comparing eqs A1 and A2 and setting them equal to zero, we get

$$k_{e_1}[A] = k_{e_2}[B] \qquad \text{(A6)}$$

If $k_{e_1} = k_{e_2}$, since A and B are formed by the chain slicing step (A-II) in equal amounts, [A] and [B]. On the other hand if $k_{e_1} \neq k_{e_2}$, the consumption rate of A and B are different, and therefore [A] ≠ [B].

Now the overall rate of production of acetic acid is given by

$$\frac{dx}{dt} = \frac{d[CH_3COOH]}{dt} = k_{f_1}[A][B] + k_{e_1}[A][ABA] + k_{e_2}[B][ABA] + k_{f_2}[AO][BO] + k_h[ABA]^2 \qquad \text{(A7)}$$

Combining eqs A1 and A6 and using simple algebraic manipulations, we get finally a rate expression for the overall acetic acid production

$$\frac{dx}{dt} = 3k_s[PET][ABA] + k_h[ABA]^2 - \left(\frac{2k_{f_1}k_{e_1}}{k_{e_2}}\right)[A]^2 \qquad \text{(A8)}$$

The only unknown in the RHS of eq A8 which cannot be experimentally measured is [A], for which a quadratic equation holds

$$k_s[PET][ABA] - \left(\frac{k_{f_1}k_{e_1}}{k_{e_2}}\right)[A]^2 - k_{e_1}[A][ABA] = 0 \qquad \text{(A9)}$$

In eq A9 only the positive root is further used in the kinetic expression A8 for the overall kinetics.

Supplementary Material Available: Textual discussion of the influence of diffusion and a table of rate constants (6 pages). Ordering information is given on any current masthead page.

References and Notes

(1) Kwolek, S. L. U.S. Patent 3.063,966, Re 30,352, 1962.
(2) Ober, C. K.; Jin, J.-I.; Lenz, R. W. *Adv. Polym. Sci.* **1984**, *59*, 103.
(3) Jackson, W. J.; Kuhfuss, H. F. *J. Polym. Sci., Polym. Chem. Ed.* **1976**, *14*, 2043. Jackson, W. J., Jr. *Proc. IUPAC, I. U. P. A. C., Macromol. Symp., 28th* **1982**, 800.
(4) Jin, J.-I.; Antoun, S.; Ober, C.; Lenz, R. W. *Br. Polym. J.* **1980**, *12*, 132.
(5) Lenz, R. W. *Faraday Discuss Chem. Soc.* **1985**, *79*, 21.
(6) Antoun, S.; Lenz, R. W.; Jin, J.-I. *J. Polym. Sci., Polym. Chem. Ed.* **1981**, *19*, 1901.
(7) Zhou, Q. F.; Lenz, R. W. *J. Polym. Sci., Polym. Chem. Ed.* **1983**, *21*, 3313.
(8) Lenz, R. W. *Polym. J.* **1985**, *17*, 105.
(9) Zhou, Q. F.; Jin, J.-I.; Lenz, R. W. *Can. J. Chem.* **1985**, *63*, 181.
(10) Galli, G.; Chiellini, E.; Ober, C. K.; Lenz, R. W. *Makromol. Chem.* **1982**, *183*, 2693.
(11) Jo, B. W.; Jin, J.-I.; Lenz, R. W. *Eur. Polym. J.* **1982**, *18*, 233.
(12) Ober, C. K.; Jin, J.-I.; Lenz, R. W. *Polym. J.* **1982**, *14*, 9.
(13) Majnusz, J.; Catala, J. M.; Lenz, R. W. *Eur. Polym. J.* **1983**, *19*, 1043.
(14) Jo, B. W.; Lenz, R. W.; Jin, J.-I. *Makromol. Chem., Rapid Commun.* **1982**, *3*, 23.
(15) Ober, C. K.; Lenz, R. W.; Galli, G.; Chiellini, E. *Macromolecules* **1984**, *16*, 1034.

(16) McFarlane, F. E.; Nicely, V. A.; Davis, T. G. In *Contemporary Topics in Polymer Science*; Pearce, E. M., Schaefgan, R. J., Eds.; Plenum Publishing Corp.: New York, 1977; Vol. 2.
(17) Blackwell, J.; Lieser, G.; Gutierrez, G. *Macromolecules* **1983**, *16*, 1418.
(18) Joseph, E.; Garth, L. W.; Baird, D. G. *Polymer* **1985**, *26*, 689.
(19) Meneczel, J.; Wunderlich, B. *J. Polym. Sci., Polym. Phys. Ed.* **1980**, *18*, 1433.
(20) Meesiri, W.; Meneczel, J.; Gaur, U.; Wunderlich, B. *J. Polym. Sci., Polym. Phys. Ed.* **1982**, *20*, 719.
(21) Zachariades, A. E.; Economy, J.; Logan, A. J. *J. Appl. Polym. Sci.* **1982**, *27*, 2009.
(22) Griffin, B. P.; Cox, M. K. *Br. Polym. J.* **1980**, *12*, 147.
(23) Sawyer, L. C. *J. Polym. Sci., Polym. Lett. Ed.* **1984**, *22*, 347.
(24) Mathew, J.; Bahulekar, R. V.; Ghadage, R. S.; Rajan, C. R.; Ponrathnam, S.; Prasad, S. D. *Macromolecules* **1992**, *25*, 7338.
(25) Hamb, F. L. *J. Polym. Sci., Polym. Chem. Ed.* **1972**, *10*, 3217.
(26) Flory, P. J. *Chem. Rev.* **1946**, *39*, 169.
(27) Steinfeld, J. I.; Francisco, J. S.; Hase, W. L. *Chemical Kinetics and Dynamics* Prentice-Hall: Englewood Cliffs, NJ, 1989.
(28) Datar, A. S.; Prasad, S. D. *Langmuir* **1991**, *7*, 1310. Datar, A. S.; Prasad, S. D.; Doraiswamy, L. K. *Ind. Eng. Chem. Res.* **1991**, *30*, 2066. Datar, A. S.; Prasad, S. D. *Ind. Eng. Chem. Res.* **1992**, *31*, 2257.
(29) Nicely, V. A.; Dougherty, J. T.; Renfro, L. W. *Macromolecules* **1987**, *20*, 573.
(30) Flory, P. J. *J. Am. Chem. Soc.* **1940**, *62*, 2261.
(31) Stupp, S. I.; Moore, J. S.; Martin, P. J. *Macromolecules* **1988**, *21*, 1228. Martin, P. J.; Stupp, S. I. *Macromolecules* **1988**, *21*, 1222. Moore, J. S.; Stupp, S. I. *Macromolecules* **1988**, *21*, 1217.
(32) Flory, P. J. *Principles of Polymer Chemistry*; Cornell University Press: Ithaca, NY, 1953.